Optimizing the Layout of Proportional Symbol Maps: Polyhedra and Computation

Guilherme Kunigami, Pedro J. de Rezende, Cid C. de Souza

Institute of Computing, University of Campinas, Campinas, SP 13083-852, Brazil,
kunigami@gmail.com, {rezende, cid}@ic.unicamp.br

Tallys Yunes

School of Business Administration, University of Miami, Coral Gables, FL 33124-8237, USA,
tallys@miami.edu

Proportional symbol maps are a cartographic tool to assist in the visualization and analysis of quantitative data associated with specific locations, such as earthquake magnitudes, oil well production, and temperature at weather stations. As the name suggests, symbol sizes are proportional to the magnitude of the physical quantities that they represent. We present two novel integer linear programming (ILP) models to solve this computational geometry problem: how to draw opaque disks on a map so as to maximize the total visible border of all disks. We focus on drawings obtained by layering symbols on top of each other, also known as *stacking drawings*. We introduce decomposition techniques, as well as several families of facet-defining inequalities which are used to strengthen the ILP models that are supplied to a commercial solver. We demonstrate the effectiveness of our approach through a series of computational experiments using hundreds of instances generated from real demographic and geophysical data sets. To the best of our knowledge, we are the first to use ILP to tackle this problem, and the first to provide provably optimal symbol maps for those data sets.

Key words: computational geometry; integer programming; cartography; symbol maps

1. Introduction

Proportional symbol maps (PSMs) are a cartographic tool to assist in the visualization and analysis of quantitative data associated with specific locations (e.g. earthquake magnitudes, oil well production, temperature at weather stations, etc.). At each location, a symbol is drawn whose size is proportional to the numerical data collected at that point on the map (Cabello et al., 2006, 2010). For our purposes, the symbols are scaled opaque disks, which are typically preferred by users (Griffin, 1990), and we focus on drawings obtained by layering symbols on top of each other, also known as *stacking drawings*. Because of overlapping, a
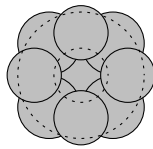
Figure 1: One cannot tell whether the bottom disk is small or large.

drawing of the disks on a plane will expose some of them (either completely or partially) and potentially obscure the others. Although there have been studies about symbol sizing, it is unclear how much the symbols on a PSM should overlap (Dent, 1999; Slocum et al., 2003). The quality of a drawing is related to how easily the user is able to correctly judge the relative sizes of the disks. Intuitively, the accuracy of such a judgment is proportional to how much of the disk borders are visible. Figure 1 illustrates why it is better to consider visible border length rather than visible area. As a consequence, the objective function consists of maximizing one of two alternative measures of quality: the minimum visible border length of any disk (the *Max-Min* problem), or the total visible border length over all disks (the *Max-Total* problem).

For n disks, Cabello et al. (2006) show that the Max-Min problem can be solved in $O(n^2 \log n)$ time in general, or in $O(n \log n)$ time if no point on the plane is covered by more than $O(1)$ disks. According to Cabello et al. (2006), the complexity of the Max-Total problem for stacking drawings is open and, therefore, we focus on this version of the problem.

The contributions of this work are: (i) identifying a new application of integer linear programming (ILP) in computational geometry and proposing two novel ILP formulations for the Max-Total problem; (ii) introducing decomposition techniques, as well as several families of facet-defining inequalities for this problem; (iii) experimenting with ILP algorithms that demonstrate the effectiveness of our approach through a series of computational tests on hundreds of instances obtained from real geophysical data from NOAA's National Geophysical Data Center (NOAA Satellite and Information Service, 2005); and (iv) providing, for the first time, provably optimal solutions to *all* of the Max-Total instances studied in Cabello et al. (2006, 2010). As a result, we find that the optimal solutions are significantly superior to the best heuristic solutions obtained with the algorithm of Cabello et al. (2006, 2010).

The PSM has a clear application to the visualization of statistical data. Good understanding of such information is crucial to strategic decisions, which is at the heart of operations research. For example, knowing the intensity and location of earthquakes is crucial in deciding where to install emergency operation centers to handle such events.

Figure 2: Arrangement with vertex v, arc r, and face f (left), and a drawing (right).

An earlier and much shorter version of some of the results herein, not including our latest and best results, appeared as Kunigami et al. (2011). We are unaware of other attempts at using ILP to solve this problem.

In Section 2, we describe the problem more formally and introduce some basic terminology. We present two alternative ILP models for the problem in Section 3, and perform a polyhedral study of those formulations in Section 4. We describe new families of facet-defining inequalities in Section 5, and introduce decomposition techniques in Section 6. The computational results obtained with ILP algorithms based on each of the two formulations appear in Section 7. Finally, we conclude the paper and propose directions for future research in Section 8. The proofs of all theoretical results presented in this paper are included in the accompanying online supplement.

2.   Problem Description and Terminology

Let $S = \{1, 2, \ldots, n\}$ be a set of disks with known radii and center coordinates on the Euclidean plane. Let $\mathcal{A}$ be the *arrangement* defined as the planar subdivision induced by the borders of all the disks in S. In other words, $\mathcal{A}$ is a partition of the Euclidean plane into regions delimited by the borders of the disks in S. A point at which two or more disk borders intersect is called a *vertex* of $\mathcal{A}$. A portion of a disk border that connects two vertices, with no other vertices in between, is called an *arc*. A region of $\mathcal{A}$ that is delimited by arcs and does not have any arcs in its interior is called a *face*. A *drawing* of S is a subset of the arcs and vertices of $\mathcal{A}$ that is drawn on top of the filled interiors of the disks in S (see Figure 2). A set of arcs on the boundary of a face that belong to the same disk constitutes a *canonical arc*. In Figure 3, the boundary of face f is made up of canonical arcs r_1 and r_2. The boundary of face g is made up of three canonical arcs: r_2, r_3 and r_4. Note that canonical arc r_4 is composed of two pieces. For simplicity, we will use the term *arc* to mean canonical arc for the remainder of the paper, unless noted otherwise.
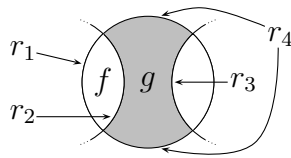
Figure 3: Three single-piece canonical arcs r_1, r_2, r_3, and a multi-piece canonical arc r_4.

Given an arrangement, many drawings are possible, but not all of them represent a sensible, physically feasible, placement of symbols. A *stacking drawing* is obtained by assigning disks to levels (a stacking order) and drawing them, in sequence, from the lowest to the highest level. Such a drawing is made up of a set of arcs A and vertices V taken from $\mathcal{A}$. An arc $r \in \mathcal{A}$ belongs to A if all the disks that contain r in their interior are assigned to levels below the level of the disk containing r in its border. Note that a visible arc of A may be the concatenation of many arcs from $\mathcal{A}$. A vertex $v \in \mathcal{A}$ belongs to V (in the sense that it is a visible point in the drawing) if and only if there exists at least one arc in A that has v as one of its endpoints.

3.   Two Alternative ILP Models

Let $G_S = (V, E)$ be an undirected graph with one vertex for every disk $i \in S$ (denoted $V(i)$) and one edge for every pair of vertices whose corresponding disks overlap. Moreover, let $m - 1$ be the length of the longest simple path in G_S, and let $\mathcal{K}$ be the set of all maximal cliques of G_S. Although G_S is a graph with special structure, the size of $\mathcal{K}$ can still be exponential in n, as is true for general graphs. This happens because a special case of these graphs are Unit Disk Graphs, which are known to have exponentially many maximal cliques in the worst case (Gupta et al., 2005).

Proposition 1. *The Max-Total problem for stacking drawings has an optimal solution that uses at most m levels.*

At first, it might seem that the number of levels needed should be no greater than the size of the largest clique in G_S. However, consider the case when G_S is a simple path with $m > 2$ vertices. The largest clique in G_S has size 2, but an optimal solution may need to use m levels. Figure 4 shows an example with $S = \{i, j, k\}$ and $m = 3$.

From the set S, its arrangement $\mathcal{A}$ can be computed in $O(n^2)$ time. Having $\mathcal{A}$, the following data, which serve as input to our ILP models, can be calculated in polynomial

Figure 4: An optimal solution (left) needs to assign the three disks to levels 1, 2, and 3, although the largest clique in G_S (right) has size 2.

time bounded by the total cardinality of all sets S_r^I, which does not exceed $O(n^3)$, in the worst case:

- $R \equiv$ set of all arcs in $\mathcal{A}$;

- $\ell_r \equiv$ length of arc $r \in R$ (total length if r has multiple pieces);

- $d_r \equiv$ disk that contains arc r in its border;

- $S_r^I \equiv$ set of disks that contain arc r in their interior.

We are now ready to describe our first model. For each $r \in R$, let the binary variable x_r be equal to 1 if arc r is visible in the drawing, and equal to 0 otherwise. Then, the objective is to maximize

$$\sum_{r \in R} \ell_r x_r \ . \tag{1}$$

We assume that $m \geq 2$ because it is trivial to find the optimal solution when $m = 1$. For each disk $i \in S$, let the binary variable y_{ip} be equal to 1 if disk i is at level p ($1 \leq p \leq m$, with 1 being the bottom level and m being the top level), and equal to 0 otherwise. A stacking drawing has to satisfy the following constraints:

$$\sum_{p=1}^{m} y_{ip} \leq 1, \qquad\qquad \forall\, i \in S \tag{2}$$

$$x_r \leq \sum_{p=1}^{m} y_{d_r p}, \qquad\qquad \forall\, r \in R \tag{3}$$

$$\sum_{i\,:\,V(i) \in K} y_{ip} \leq 1, \qquad\qquad \forall\, 1 \leq p \leq m,\ K \in \mathcal{K} \tag{4}$$

$$\sum_{a=1}^{p} y_{d_r a} + \sum_{b=p}^{m} y_{ib} + x_r \leq 2, \qquad\qquad \forall\, r \in R,\ i \in S_r^I,\ 1 \leq p \leq m \tag{5}$$

$$x_r \in \{0, 1\}, \qquad\qquad \forall\, r \in R \tag{6}$$

$$y_{ip} \in \{0, 1\}, \qquad\qquad \forall\, i \in S,\ 1 \leq p \leq m \tag{7}$$

We refer to the convex hull of feasible integer solutions to (2)–(7) as P_1. Constraint (2) states that each disk is assigned to at most one level. Due to Proposition 1 and because assigning a disk to the lowest level never decreases the objective function value, any optimal solution to (2)–(7) can be converted to another solution with the same value and having all disks assigned to at most m levels. Hence, we use $\leq$ instead of $=$ in (2) to prevent P_1 from losing dimension, turning the study of the facial structure of this polytope (see Section 4) technically simpler. Constraint (3) states that a disk with a visible arc must be assigned to a level, and (4) says that overlapping disks can not be at the same level. Although the latter constraints can be exponential in number, a compact formulation can be easily obtained by replacing them with simple constraints stating that a disk cannot be simultaneously on two different levels. However, we prefer to present the stronger form of constraints (4) which derives directly from previous studies on the independent set polytope (see Padberg, 1973). Constraint (5) ensures that arc r is only visible if d_r is above all other disks that contain r.

Our second model is related to the partial order polytope (Müller, 1996) (see Section 5 for further details). It uses the same x_r variables introduced in the first model, but replaces variables y_{ip} with new binary variables w_{ij} for every pair of distinct disks $i, j \in S$. If $w_{ij} = 1$, it means that disk i is placed above disk j. The constraints are as follows:

$$w_{ij} + w_{ji} \leq 1, \qquad\qquad \forall\, i, j \in S,\ i < j \qquad (8)$$

$$x_r \leq w_{d_r j}, \qquad\qquad \forall\, r \in R,\ j \in S_r^I \qquad (9)$$

$$w_{ij} + w_{jk} - w_{ik} \leq 1, \qquad\qquad \forall\, i, j, k \in S,\ i \neq j \neq k \neq i \qquad (10)$$

$$x_r \in \{0, 1\}, \qquad\qquad \forall\, r \in R \qquad (11)$$

$$w_{ij} \in \{0, 1\}, \qquad\qquad \forall\, i, j \in S,\ i \neq j \qquad (12)$$

We refer to the convex hull of feasible integer solutions to (8)–(12) as P_2. Constraint (8) states that either i is above j, or vice-versa. Constraint (9) states that if arc r is visible, its disk d_r has to be above all other disks that contain r in their interior. Finally, (10) makes sure that the (partial) order imposed by the w_{ij} variables is transitive.

Note that both formulations accept partial drawings as feasible solutions. By a partial drawing we mean a set of arcs that is a subset of a drawing. However, because our objective is to maximize a linear function with non-negative coefficients, any optimal solution to these models must be a complete drawing.

4.   Polyhedral Results

In this section, we obtain the dimension of P_1 and P_2, and determine which inequalities in their original formulations define facets.

4.1.   Polyhedral Study of P_1

Proposition 2. *The dimension of P_1 is $nm + |R|$.*

Proposition 3. *Given an arc $r \in R$, the inequality $x_r \geq 0$ defines a facet of P_1, whereas the inequality $x_r \leq 1$ does not.*

Proposition 4. *Given a disk $i \in S$, and a level $1 \leq p \leq m$, the inequality $y_{ip} \geq 0$ defines a facet of P_1, whereas the inequality $y_{ip} \leq 1$ does not.*

Proposition 5. *Given a disk $i \in S$, (2) defines a facet of P_1.*

Proposition 6. *Given an arc $r \in R$, (3) defines a facet of P_1.*

Proposition 7. *Given $1 \leq p \leq m$ and $K \in \mathcal{K}$ with $|K| \geq 2$, (4) defines a facet of P_1.*

Proposition 8. *Given an arc $r \in R$, $i \in S_r^I$ and $1 \leq p \leq m$, (5) does not define a facet of P_1, but (13) does if $1 \leq p < m$.*

$$\sum_{a=1}^{p} y_{d_r a} + \sum_{b=p}^{m} y_{ib} + x_r \leq 1 + \sum_{a=1}^{m} y_{d_r a} \tag{13}$$

4.2.   Polyhedral Study of P_2

Proposition 9. *The dimension of P_2 is $n(n-1) + |R|$.*

Proposition 10. *Given an arc $r \in R$, the inequality $x_r \geq 0$ defines a facet of P_2, whereas the inequality $x_r \leq 1$ defines a facet of P_2 only when $S_r^I = \emptyset$.*

Proposition 11. *Given two distinct disks $i, j \in S$, the inequality $w_{ij} \geq 0$ defines a facet of P_2 if $S_r^I = \emptyset$ for all arcs r on the border of disk i. Moreover, the inequality $w_{ij} \leq 1$ does not define a facet of P_2.*

Proposition 12. *Given two disks $i, j \in S$ with $i < j$, (8) defines a facet of P_2.*

Proposition 13. *Given an arc $r \in R$ and a disk $j \in S_r^I$, (9) defines a facet of P_2.*

Proposition 14. *Given three distinct disks $i, j, k \in S$, (10) defines a facet of P_2.*

4.3.   Relationship Between P_1 and P_2

We conclude this section with a formal comparison of our two ILP formulations. Let $\widetilde{P}_1$ be the feasible set of the linear relaxation of (2)–(7) and let $\widetilde{P}_2$ be the feasible set of the linear relaxation of (8)–(12). Moreover, let $\widetilde{P}_1^x$ and $\widetilde{P}_2^x$ be the projections of $\widetilde{P}_1$ and $\widetilde{P}_2$ onto the x-space, respectively. More specifically, $\widetilde{P}_1^x = \{x \in \mathbb{R}^{|R|} \,|\, (y, x) \in \widetilde{P}_1 \text{ for some } y \in \mathbb{R}^{nm}\}$ and $\widetilde{P}_2^x = \{x \in \mathbb{R}^{|R|} \,|\, (w, x) \in \widetilde{P}_2 \text{ for some } w \in \mathbb{R}^{n(n-1)}\}$.

Proposition 15. $\widetilde{P}_1^x \nsubseteq \widetilde{P}_2^x$.

We conjecture that $\widetilde{P}_2^x \subset \widetilde{P}_1^x$, but we do not have a proof of that yet.

5.   Strengthening the ILP Formulations

The geometric nature of PSMs enables us to obtain new valid inequalities by observing that certain groups of arcs cannot be visible simultaneously due to a physical impossibility. In the sequel, $\mathcal{A}$ is an arrangement of disks on a plane. We use the following additional data sets:

- $D_f \equiv$ set of disks that contain face f.

- $B_f \equiv$ set of arcs that form the boundary of face f. $B_f^+ = \{r \in B_f \,|\, d_r \in D_f\}$ and $B_f^- = B_f \setminus B_f^+$.

- $I_f \equiv$ set of disks whose borders contain an arc in B_f.

- $C_f \equiv$ set of disks that contain face f in their interior ($C_f = D_f \setminus I_f$).

Consider the arrangement in Figure 3. The boundary of face g is formed by arcs r_2, r_3, and r_4. We have $B_g = \{r_2, r_3, r_4\}$, $D_g = \{d_{r_4}\}$, $B_g^+ = \{r_4\}$, $B_g^- = \{r_2, r_3\}$, $I_g = \{d_{r_2}, d_{r_3}, d_{r_4}\}$, and $C_g = \emptyset$.

   In the arrangement of Figure 5, the boundary of face f is formed by arcs r_1, r_2, and r_3. Therefore, we have $B_f = B_f^+ = \{r_1, r_2, r_3\}$, $D_f = \{d_{r_1}, d_{r_2}, d_{r_3}, d_{r_4}\}$, $I_f = \{d_{r_1}, d_{r_2}, d_{r_3}\}$, and $C_f = \{d_{r_4}\}$. If one of the arcs in B_f is visible in a drawing, the other two cannot be visible. Moreover, if d_{r_4} is assigned to the topmost level m, f will not be visible. This leads to the valid inequality $y_{d_{r_4}m} + x_{r_1} + x_{r_2} + x_{r_3} \leq 1$. In general, we have the following result:
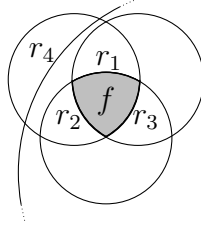
Figure 5: Arcs r_1, r_2, and r_3 of face f cannot be visible simultaneously.

Proposition 16. *Let f be a face of $\mathcal{A}$ with $|B_f^+| \geq 1$. If $|C_f| \geq 1$ or $|B_f^+| \geq 2$, then (14) defines a facet of P_1.*

$$\sum_{i \in C_f} y_{im} + \sum_{r \in B_f^+} x_r \leq 1 \tag{14}$$

Proposition 17. *Let f be a face of $\mathcal{A}$ with $|B_f^-| \geq 1$. For each $r \in B_f^-$, (15) defines a facet of P_1.*

$$\sum_{i \in D_f} y_{im} + x_r \leq 1 \tag{15}$$

Now let G_R be a graph with one node for every arc $r \in R$, denoted $V(r)$, and an edge between two nodes $V(r_1)$ and $V(r_2)$ if $d_{r_1} \in S_{r_2}^I$ and $d_{r_2} \in S_{r_1}^I$ (i.e. r_1 and r_2 cannot be visible simultaneously). Given a clique K of G_R, to simplify notation we will treat K as a set of arcs whose corresponding vertices induce a clique in G_R. Therefore, we can apply typical set operations to K, such as writing $r \in K$ to indicate that $V(r)$ is a node of the clique, and writing $|K|$ to indicate the number of nodes in the clique.

In an attempt to find the counterpart of Proposition 16 for P_2, we obtained the following result.

Proposition 18. *Let K be a maximal clique in G_R with $|K| \geq 3$. Then, (16) defines a facet of P_2.*

$$\sum_{r \in K} x_r \leq 1 \tag{16}$$

Because the w_{ij} variables define a partial order on the disks in S, P_2 can be viewed as a lifted partial order polytope (POP) with side constraints (Müller, 1996). Therefore, one
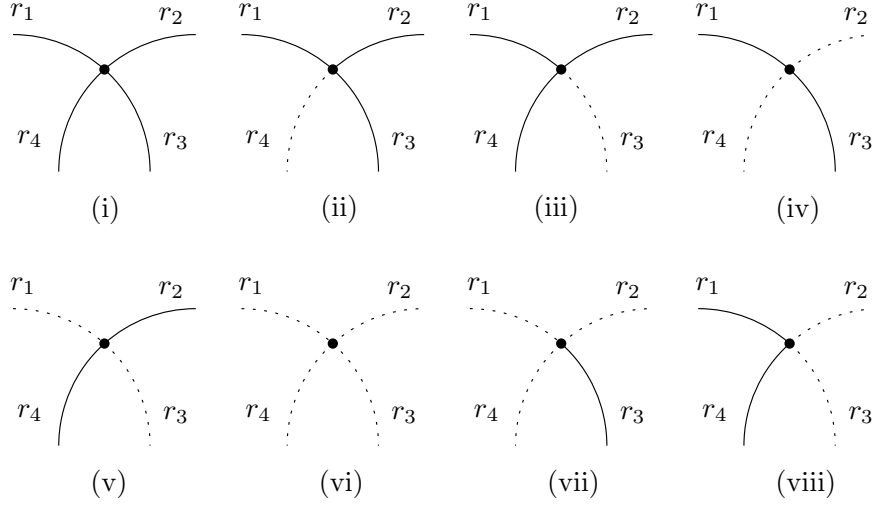
9

Figure 6: A non-degenerate vertex (i), five feasible arc configurations: (ii)–(vi), and two infeasible ones: (vii) and (viii).

could use valid inequalities for the POP as a starting point for finding valid inequalities for P_2. The odd closed walk inequality studied in Müller (1996) is one such example.

Proposition 19. *Let $D_S = (V, A)$ be a complete directed graph with one node in V for every disk in S. As before, $V(i)$ denotes the node corresponding to disk i, and an arc from $V(i)$ to $V(j)$ in D_S corresponds to the variable w_{ij}. Let $C = (V(i_1), \ldots, V(i_k), V(i_{k+1}))$, with $i_{k+1} = i_1$ and $i_{k+2} = i_2$, be an odd cycle of length k in D_S. Then, (17) defines a facet of P_2.*

$$\sum_{a=1}^{k} w_{i_a i_{a+1}} - \sum_{a=1}^{k} w_{i_a i_{a+2}} \leq \frac{k-1}{2} \tag{17}$$

A vertex of an arrangement is *non-degenerate* if it is an intersection point of exactly two disks or, equivalently, four arcs, as shown in Figure 6(i). Since each arc can be either visible or not, there are 16 potential assignments of values to their respective x variables. Due to our objective function (1), drawings that are candidates for optimal solutions can only include the five assignments shown in Figure 6(ii)–(vi) (dashed arcs are obscured). Assignments such as the ones shown in Figure 6(vii)–(viii) cannot be part of an optimal drawing. This observation gives rise to inequalities (18)–(21). Because the definitions of P_1 and P_2 accept partial drawings as feasible solutions, (18)–(21) are not strictly valid for P_1 and P_2. Nevertheless, since optimal solutions are complete drawings that never violate (18)–(21), these inequalities can still be used to speed up the search.
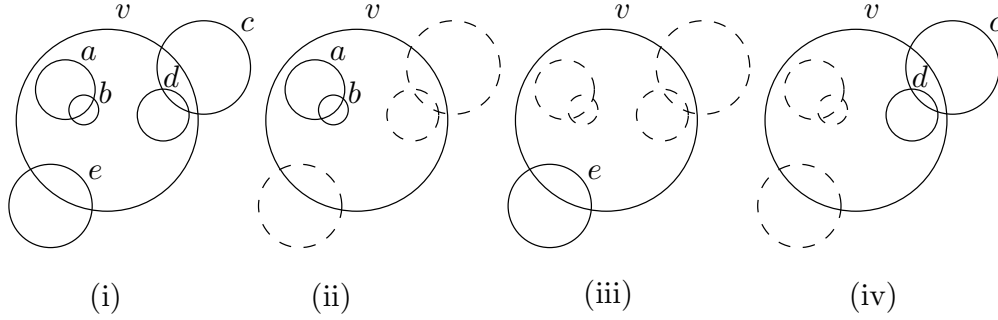
Figure 7: An instance that allows for decomposition.

$$x_{r_1} \geq x_{r_3} \tag{18}$$

$$x_{r_2} \geq x_{r_4} \tag{19}$$

$$x_{r_3} + x_{r_4} \geq x_{r_1} \tag{20}$$

$$x_{r_3} + x_{r_4} \geq x_{r_2} \tag{21}$$

6.   Decomposition Techniques

To reduce the size of the ILP model, we introduce decomposition techniques that allow us to consider smaller sets of disks at a time.

Without loss of generality, we assume that G_S is connected. Otherwise, each of its connected components can be treated separately. A graph is 2-connected if it cannot be disconnected by removing less than 2 vertices. When the graph is connected but not 2-connected, the disconnecting vertices are known as a *cut vertices*, or *articulation points* (West, 2001). If G_S is not 2-connected, we can decompose it around its articulation points. Consider the example in Figure 7(i), in which $S = \{a, b, c, d, e, v\}$. The node corresponding to disk v, i.e. $V(v)$, is an articulation point of G_S because its removal disconnects the graph into three connected components: $\{a, b\}$, $\{c, d\}$, and $\{e\}$. By adding v to each of these components, we get instances (ii), (iii), and (iv) of Figure 7, which are solved independently. Those three optimal solutions can be combined into an optimal solution for the entire set S by preserving the relative order of the disks in each solution. Proposition 20 formalizes this idea.

Proposition 20. *Let S be a set of disks such that G_S is not 2-connected and let v be a disk corresponding to an articulation point of G_S. Let S_k contain v plus the disk set of the k-th connected component obtained after the removal of $V(v)$ from G_S. The optimal solutions for each S_k can be combined into an optimal solution for S in polynomial time.*

11

If the graph of a connected component (G_{S_k}) is not 2-connected and has an articulation point, the above procedure can be applied recursively.

From Figure 7(ii), it is clear that there exists an optimal solution in which a and b are drawn above v. Hence, we can consider a and b as a separate instance, and v as another. Proposition 21 formalizes this idea.

Proposition 21. *Let S be a set of disks and let H_S be a directed graph with one node for every disk in S and an arc from node i to node j whenever a portion of the border of i's disk is contained in the interior of j's disk. Let S_k be the disk set of the k-th strongly connected component of H_S. The optimal solutions for each S_k can be combined into an optimal solution for S in polynomial time.*

7.   Computational Experiments

Our experiments are performed on the same set of instances used in Cabello et al. (2006). Instances *City 156* and *City 538* represent the 156 and 538 largest American cities, respectively, in which the area of each disk is proportional to the city's population. Instances *Deaths* and *Magnitudes* represent the death count and Richter scale magnitude of 602 earthquakes worldwide, respectively. Disks are placed at the epicenters of each earthquake, and disk areas are proportional to the corresponding quantities (NOAA Satellite and Information Service, 2005). When disks in an instance coincide, we replace them by a single disk whose border is the total border length of the original disks. This is possible because we can assume that such disks would occupy adjacent levels in an optimal solution. This pre-processing step reduces the number of disks in *Deaths* and *Magnitudes* to 573 and 491, respectively.

Part of the success of our approach depends on using our decomposition techniques to break down those large original instances into hundreds of smaller instances, as explained next.

In Table 1, column *Connected* shows the number of connected components in G_S for each instance, with the number of disks in the largest component in parentheses. Column *Strongly Connected* shows the resulting number of components (and largest component) after we apply the decomposition of Proposition 21. Proposition 20 yields further decomposition, as shown under column *2-Connected.* The reductions in problem size are remarkable. *City 538* can now be solved by optimizing over sets of disks no larger than one tenth of its original size. Before applying our decompositions, the largest instance in the original data

Table 1: Number of components and largest component before/after decomposition.

Instance	# Disks	Connected	Strongly Connected	2-Connected
City 156	156	38 (57)	45 (56)	53 (29)
City 538	538	185 (98)	213 (94)	240 (53)
Deaths	573	134 (141)	317 (85)	333 (70)
Magnitudes	491	31 (155)	31 (155)	45 (116)

set had 573 disks. As shown in the rightmost column of Table 1, the largest instance after decomposition has 116 disks. Solving the original instances is now equivalent to solving 671 significantly smaller instances.

We solved the strengthened versions of the two ILP models described in Section 3 with a commercial solver running its standard branch-and-cut algorithm. Thus, the cuts that are separated during the execution of the algorithm are restricted to those already implemented inside the solver. From now on, we refer to the first model ((2)–(7)) as model M_1, and we refer to the second model ((8)–(12)) as model M_2. We now present some implementation details for each case.

In model M_1, we implement (2) as SOS1, substitute (13) for (5), and add (14), (18)–(21) at the root node. (Inequalities (15) did not help computationally.) Because $|\mathcal{K}|$ can be exponentially large, rather than including all of (4), we heuristically look for an edge covering of G_S by maximal cliques (Nemhauser and Sigismondi, 1992). Alternatively, we also tried replacing (4) with $y_{ip} + y_{jp} \leq 1$ for each level p and all $(i,j) \in E$. Although theoretically weaker, the latter formulation performed better in our experiments. This might be explained by the sparser coefficient matrix of the weaker model, which typically yields easier-to-solve linear relaxations. Finally, instead of computing the exact value of m as in Proposition 1, which is NP-Hard (Garey and Johnson, 1979), we use $m = n$ in every run, because the exact m is equal to n in many of the large components.

In model M_2, we create a variable w_{ij} for all pairs $i, j \in S$ with $i \neq j$. This way, (10) prevents any cyclic orientation among disks. In addition, we implement (8) as an equality rather than an inequality because our computational experience suggests that the equality form yields better running times. Finally, we include (16) and (18)-(21) at the root node. For (16) in particular, instead of looking for all maximal cliques in G_R as described in Proposition 18, we only consider cliques corresponding to the arcs of B_f^+ for each face f of the arrangement. Although such cliques are not necessarily maximal, they can be found efficiently and already provide good results (see below).

Table 2: Average results with model M_1 over smallest non-trivial components of each instance.

Original Instance	Comp. w/ $\lvert S_k \rvert > 2$	$\lvert S_k \rvert$			Nodes			Time (in sec.)		
		Min	Avg	Max	Min	Avg	Max	Min	Avg	Max
City 156	11	3	5.3	14	1	20.8	213	0	3.5	38
City 538	20	3	5.4	12	1	11.9	145	0	0.4	5
Deaths	22	3	4.7	10	1	5.8	93	0	0.1	1
Magnitudes	14	3	4.7	10	1	1.8	7	0	0.1	1

Our implementation was done in C++, using CGAL for data extraction (Wein et al., 2007). We use *XPRESS-Optimizer* (Fair Isaac Corporation, 2009) version 20.00 to solve each problem on a 2.4GHz Intel® Core™2 Quad processor, with 4GB of RAM. Unless noted otherwise, we limit each run to five hours of CPU time.

For comparison purposes, we use the $O(n^2 \log n)$ heuristic from Cabello et al. (2006, 2010) to find good feasible solutions. Despite being a Max-Min heuristic, its solutions also perform well in terms of the Max-Total objective.

7.1. Results Obtained with Model M_1

Out of the 671 components obtained through decomposition, all but the five or six largest ones from each original instance are easily solved by our optimization algorithm. We will focus on them first.

For components with $\lvert S_k \rvert \leq 2$, the solution is trivial. For the remaining easy-to-solve components, we summarize our results in Table 2. Column *Comp. w/ $\lvert S_k \rvert > 2$* indicates how many easy components from the corresponding original instance have more than two disks. The next nine columns indicate the minimum, average, and maximum values of component size, followed by the number of search nodes and CPU time required to find an optimal solution, respectively. When compared to the heuristic solutions, the optimal solutions to the 67 problems from Table 2 are 13.2% better on average (min = 0% and max = 158.4%).

The results obtained with the five (or six) most challenging components of each original instance appear in Table 3. Component names are written as "α-β-γ (δ)", where α identifies the instance, β-γ indicates that this is the γ-th component generated by Proposition 20 when applied to the β-th component generated by Proposition 21, and δ is the number of disks. In Table 3, *Base Value* represents the total length of arcs r that are visible in any feasible solution ($S_r^I = \emptyset$). This value is equal to the length of the border of the region

Table 3: Results with model M_1 on largest components from each original problem instance.

Component	Base Value	Best Feasible	Best UB	% Gap	% Above Heur.	Nodes	Time (s)
156-18-0 (7)	63.97	**12.91**	**12.91**	0	0	1	0
156-3-2 (8)	39.84	**40.99**	**40.99**	0	8.5	7	0
156-3-0 (14)	66.15	**71.17**	**71.17**	0	7.8	213	39
156-2-0 (26)	167.22	**138.05**	**138.05**	0	3.1	5949	381
156-2-1 (29)	219.36	**153.85**	**153.85**	0	1.4	117	10
538-47-2 (17)	26.75	**25.27**	**25.27**	0	2.0	2463	1259
538-3-0 (26)	34.27	**39.19**	**39.19**	0	15.0	23589	9562
538-29-1 (26)	46.48	**36.40**	**36.40**	0	4.3	1143	1260
538-1-6 (29)	21.98	43.51	47.05	8.0	9.6	2399	18000
538-1-0 (51)	77.37	82.13	107.35	30.7	0.0	22	18000
538-24-0 (53)	18.98	58.50	186.23	218.3	0.0	1	18000
death-6-0 (12)	953.08	**60.16**	**60.16**	0	0.0	51	1
death-8-0 (14)	68.05	**39.65**	**39.65**	0	3.1	87	0
death-0-0 (24)	175.78	**145.74**	**145.74**	0	5.7	4925	199
death-3-0 (24)	441.75	**323.18**	**323.18**	0	1.3	3919	210
death-2-0 (70)	725.28	964.66	1652.02	71.2	0.0	1	18000
mag-5-1 (25)	214.92	**593.74**	**593.74**	0	3.7	965	9609
mag-6-0 (26)	217.21	579.58	610.99	5.4	5.0	3385	18000
mag-1-1 (39)	417.32	919.28	1350.23	46.9	0.0	3	18000
mag-5-0 (81)	601.79	1741.24	2317.66	33.1	0.0	1	18000
mag-1-0 (113)	581.41	2743.68	-	-	0.0	1	18000
mag-7-0 (116)	700.37	2622.46	-	-	0.0	1	18000

corresponding to the union of all disks and is subtracted from the solution values in the remaining columns. *Best Feasible* and *Best UB* are the best lower and upper bounds on the optimal value found within the time limit, respectively (optimal solutions appear in bold). Column *% Gap* shows the relative difference between the lower and upper bounds, and *% Above Heur.* indicates how much better the best known lower bound is with respect to the heuristic solution discussed above (*% Above Heur.* = [(best solution by M_1) − (best heuristic solution)]/(best heuristic solution)).

Instance *City 156* presented no difficulties, having all of its five largest components solved in less than 8 minutes. We found optimal or near optimal solutions to the first four of the largest components of *City 538*, with significant improvements in quality with respect to the heuristic solutions. The two largest components of *City 538* turned out to be more challenging, with sizable gaps remaining after five hours of computation. All but one of the largest earthquake death components were solved to optimality. As was the case

15

Table 4: Number of arcs and size of ILP formulation for the 5 largest components using model M_1.

Component	# Disks	# Arcs	# Cols.	# Rows before cuts	# Rows after cuts
538-24-0	53	3753	6562	3026565	3035839
death-2-0	70	1366	6266	620970	624115
mag-5-0	81	2059	8620	914490	919623
mag-1-0	113	4318	17087	3733407	3744116
mag-7-0	116	3759	17215	2792468	2801845

with component 538-24-0, the time limit was exhausted during the solution of death-2-0 even before branching started. The largest components obtained from the decomposition of earthquake magnitudes turned out to be the most challenging ones. Note that we do not have valid upper bounds for instances mag-1-0 and mag-7-0 because the time limit was not even enough to solve their first linear relaxation. Overall, we were able to find optimal solutions to 662 out of the 671 components derived from our original four instances.

Cutting planes (14) and (18)–(21) were essential in achieving the results in Table 2 and Table 3. With those cuts, the number of search nodes was 54 times smaller on average, with some cases achieving reductions of almost three orders of magnitude. (Five of the 21 hardest components — six overall — would not have been solved to optimality by model M_1 without those cuts.) As a consequence, computation times were also drastically reduced.

Because of its direct relationship to the amount of overlapping between disks, the number of arcs in an instance/component is a better measure of difficulty than the number of disks. Model M_1 appears to be capable of handling about 600 to 700 arcs in five hours of CPU which, for our benchmark set, roughly corresponds to instances having between 24 and 26 disks. Table 4 contains more details about the size of our five largest components and how big their ILP formulation is before and after the inclusion of cuts. Because the number of cuts is small in model M_1, we add them at the root node of the search tree.

7.2.   Results Obtained with Model M_2

As far as size is concerned, model M_2 is roughly equivalent to model M_1 in terms of the number of variables, but it can have much fewer constraints than model M_1, depending on the problem instance. For the instances listed in Table 4, for example, model M_2 can have between 1.6 and 14.7 times fewer rows than model M_1. Moreover, the number of non-zero entries in the constraint matrices of those instances can be between 45 and 288 times smaller

Table 5: Results with model M_2 on components not solved to optimality by model M_1.

Component	Base Value	Best Feasible	Best UB	% Gap	% Above Heur.	Nodes	Time (s)
538-1-6 (29)	21.98	**44.32**	**44.32**	0	11.7	1	5
538-1-0 (51)	77.37	**90.08**	**90.08**	0	9.7	1	19
538-24-0 (53)	18.98	**65.08**	**65.08**	0	11.2	453	84308
death-2-0 (70)	725.28	**1152.13**	**1152.13**	0	19.4	1	61
mag-6-0 (26)	217.21	**579.58**	**579.58**	0	5.0	1	13
mag-1-1 (39)	417.32	**1128.52**	**1128.52**	0	22.8	1	48
mag-5-0 (81)	601.79	**1914.28**	**1914.28**	0	9.9	1	2312
mag-1-0 (113)	581.41	**3158.82**	**3158.82**	0	15.1	1	34306
mag-7-0 (116)	700.37	**2916.17**	**2916.17**	0	11.2	1	25256

in model M_2.

For our set of problem instances, model M_2 turns out to be empirically superior to model M_1. On average, for the easy-to-solve instances (i.e. those summarized in Table 2), model M_2 solves 3.7 times faster (min = 0.95 times, max = 90 times) than model M_1, and uses 9 times fewer (min = 1 times, max = 213 times) search nodes to reach optimality. However, the most impressive results are obtained on the larger, unsolved components of Table 3, as can be seen in Table 5. Model M_2 managed to solve all remaining instances to optimality, five of them quite easily. Although we allowed it to run for more than 5 hours in some cases, it is important to note that model M_1 would not have been able to solve those instances even if it had been given the same amount of additional time.

While comparing the root node upper bounds for the instances in Table 5 for which both models found a valid upper bound (i.e. excluding mag-1-0 and mag-7-0), we verified that the bounds obtained from model M_2 are always strictly better (10.4% better on average; 17.0% better if we ignore the base value) than those from model M_1. Although our implementation of constraints (4), (8), and (16) varies slightly from their strict definitions (see Section 7), the above results, coupled with the superior empirical performance of model M_2, as well as Proposition 15, are supportive of the conjecture stated at the end of Section 4.

8.   Conclusions

We propose two novel ILP formulations to optimize stacking drawings of proportional symbol maps (PSMs) with the objective of maximizing the total visible border of its symbols (opaque disks in our case). By studying structural and polyhedral aspects of these formulations, we

devised effective decomposition techniques and new families of facet-defining inequalities that greatly reduce the computational effort required to solve the problem. These improvements enabled us to find the first provably optimal solutions to all of the real-world instances studied in Cabello et al. (2006, 2010). Because PSM instances are still challenging to solve when the number of arcs exceeds 2000 or so, we continue to study the PSM polyhedron in search of new families of cutting planes and/or alternative formulations.

Acknowledgments

References

Cabello, S., H. Haverkort, M. van Kreveld, B. Speckmann. 2006. Algorithmic aspects of proportional symbol maps. Y. Azar, T. Erlebach, eds., *Proceedings of the 14th European Symposium on Algorithms (ESA)*, *Lecture Notes in Computer Science*, vol. 4168. Springer-Verlag, 720–731.

Cabello, S., H. Haverkort, M. van Kreveld, B. Speckmann. 2010. Algorithmic aspects of proportional symbol maps. *Algorithmica* **58** 543–565.

Cormen, T. H., C. E. Leiserson, R. L. Rivest, C. Stein. 2001. *Introduction to Algorithms*. 2nd ed. MIT Press.

Dent, B. 1999. *Cartography – Thematic Map Design*. 5th ed. McGraw-Hill.

Fair Isaac Corporation. 2009. *Xpress Optimizer Reference Manual*.

Garey, M. R., D. S. Johnson. 1979. *Computers and Intractability*. Freeman, San Francisco.

Griffin, T. 1990. The importance of visual contrast for graduated circles. *Cartography* **19** 21–30.

Gupta, R., J. Walrand, O. Goldschmidt. 2005. Maximal cliques in unit disk graphs: Polynomial approximation. *Proceedings of the Second International Network Optimization Conference (INOC)*. Lisbon, Portugal. Available at: `http://citeseerx.ist.psu.edu/viewdoc/download?doi=10.1.1.70.1687&rep=rep1&type=pdf`.

Kunigami, G., P. J. de Rezende, C. C. de Souza, T. Yunes. 2011. Optimizing the layout of proportional symbol maps. B. Murgante et al., ed., *Proceedings of the ICCSA, Part III, 11th International Workshop on Computational Geometry and Applications (CGA)*, *Lecture Notes in Computer Science*, vol. 6784. Springer-Verlag, 1–16.

Müller, R. 1996. On the partial order polytope of a digraph. *Mathematical Programming* **73** 31–49.

Nemhauser, G. L., G. Sigismondi. 1992. A strong cutting plane/branch-and-bound algorithm for node packing. *Journal of the Operational Research Society* **43** 443–457.

Nemhauser, G. L., L. A. Wolsey. 1988. *Integer and combinatorial optimization*. Wiley-Interscience, New York, NY, USA.

NOAA Satellite and Information Service. 2005. National geophysical data center. `http://www.ngdc.noaa.gov`.

Padberg, M. W. 1973. On the facial structure of set packing polyhedra. *Mathematical Programming* **5** 199–215.

Slocum, T. A., R. B. McMaster, F. C. Kessler, H. H. Howard. 2003. *Thematic Cartography and Geographic Visualization*. 2nd ed. Prentice Hall.

Wein, R., E. Fogel, B. Zukerman, D. Halperin. 2007. Advanced programming techniques applied to CGAL's arrangement package. *Computational Geometry* **38** 37–63. `http://www.cgal.org`.

West, D. 2001. *Introduction to Graph Theory*. 2nd ed. Prentice Hall.

Online supplement for the paper "Optimizing the Layout of Proportional Symbol Maps: Polyhedra and Computation".

Guilherme Kunigami, Pedro J. de Rezende, Cid C. de Souza

Institute of Computing, University of Campinas, Campinas, SP 13083-852, Brazil,
kunigami@gmail.com, {rezende, cid}@ic.unicamp.br

Tallys Yunes

School of Business Administration, University of Miami, Coral Gables, FL 33124-8237, USA,
tallys@miami.edu

A.1.　Introduction

This document contains the proofs of the propositions presented in the main body of our paper. For ease of reference, we reproduce below both sets of inequalities defining the two models for the PSM problem given in Section 3.

$$\sum_{p=1}^{m} y_{ip} \leq 1, \qquad\qquad \forall\, i \in S \qquad (2)$$

$$x_r \leq \sum_{p=1}^{m} y_{d_r p}, \qquad\qquad \forall\, r \in R \qquad (3)$$

$$\sum_{i\,:\,V(i)\in K} y_{ip} \leq 1, \qquad\qquad \forall\, 1 \leq p \leq m,\ K \in \mathcal{K} \qquad (4)$$

$$\sum_{a=1}^{p} y_{d_r a} + \sum_{b=p}^{m} y_{ib} + x_r \leq 2, \qquad\qquad \forall\, r \in R,\ i \in S_r^I,\ 1 \leq p \leq m \qquad (5)$$

$$x_r \in \{0,1\}, \qquad\qquad \forall\, r \in R \qquad (6)$$

$$y_{ip} \in \{0,1\}, \qquad\qquad \forall\, i \in S,\ 1 \leq p \leq m \qquad (7)$$

We refer to the convex hull of all feasible integer solutions to (2)–(7) as P_1.

$$w_{ij} + w_{ji} \leq 1, \qquad\qquad \forall\, i, j \in S,\ i < j \qquad\qquad (8)$$

$$x_r \leq w_{d_r j}, \qquad\qquad \forall\, r \in R,\ j \in S_r^I \qquad\qquad (9)$$

$$w_{ij} + w_{jk} - w_{ik} \leq 1, \qquad\qquad \forall\, i, j, k \in S,\ i \neq j \neq k \neq i \qquad\qquad (10)$$

$$x_r \in \{0, 1\}, \qquad\qquad \forall\, r \in R \qquad\qquad (11)$$

$$w_{ij} \in \{0, 1\}, \qquad\qquad \forall\, i, j \in S,\ i \neq j \qquad\qquad (12)$$

We refer to the convex hull of all feasible integer solutions to (8)–(12) as P_2.

In each proof, the vector $\vec{x}$ contains all of the variables in the formulation under consideration. Specifically, in proofs related to P_1, $\vec{x} = (y, x) \in \mathbb{R}^{nm+|R|}$, whereas in proofs related to P_2, $\vec{x} = (w, x) \in \mathbb{R}^{n(n-1)+|R|}$.

To prove that a given valid inequality $\beta\vec{x} \leq \beta_0$ defines a facet of P_1 or P_2, we follow one of two methods: (i) the *direct method* in which we list the required number of affinely independent points satysfying $\beta\vec{x} = \beta_0$; or (ii) the *indirect method* discussed in Theorem 3.6, Part I.4 of Nemhauser and Wolsey (1988), which works as follows. (We will focus on P_1, but the same explanation is also valid for P_2.) Let F be the face of P_1 induced by $\beta\vec{x} \leq \beta_0$, that is $F = \{\vec{x} \in P_1 \mid \beta\vec{x} = \beta_0\}$ ($F \neq \emptyset$ and $F \neq P_1$ in all of our proofs). Let $\pi\vec{x} \leq \pi_0$ be a generic valid inequality for P_1 whose induced face contains F. Because P_1 is full-dimensional, if we can show that $\pi\vec{x} \leq \pi_0$ is a scalar multiple of $\beta\vec{x} \leq \beta_0$, the latter inequality must define a facet of P_1. This is accomplished by adequately choosing points $\vec{x}_0 \in F$ and requiring that π and π_0 be such that $\pi\vec{x}_0 = \pi_0$ as well. After enough such points are considered, the values of π and π_0 can be calculated by solving a system of equations. For $\beta\vec{x} \leq \beta_0$ to be facet-defining, the solution of this system must be of the form $\pi = \alpha\beta$ and $\pi_0 = \alpha\beta_0$, for some scalar α.

To construct the points $\vec{x}_0 \in F$ for use in indirect-method proofs, we set some of their coordinates to specific values to guarantee feasibility. All the coordinates that are not assigned specific values inside a proof are always assumed to be equal to zero, unless noted otherwise.

Finally, before proceeding to the proofs, we need to clarify the indexation of vector π when it is used in inner products of the form $\pi\vec{x}$, where $\vec{x}$ is a specifically constructed feasible solution (akin to $\vec{x}_0$ in the previous paragraph). In proofs related to P_1, π_{ip} is the component of π that multiplies variable y_{ip}, and π_r is the component that multiplies variable

x_r. In proofs related to P_2, π_{ij} is the component of π that multiplies variable w_{ij}, and π_r is again the component that multiples variable x_r.

Proposition 1. *The Max-Total problem for stacking drawings has an optimal solution that uses at most m levels.*

Proof. Given an optimal solution, create a directed graph G'_S such that $V(G'_S) = V(G_S)$ and arc (i, j) is directed from i to j in G'_S if edge $(i, j) \in E(G_S)$ and disk i is at a level below disk j. Because the solution is a stacking drawing, G'_S is a directed acyclic graph (DAG). Therefore, G'_S admits a *topological ordering* of its vertices (Cormen et al., 2001), that is, an assignment of its vertices to numbered layers such that, whenever a directed arc from i to j exists, i's layer has a smaller number than j's layer. Note that this ordering induces the same stacking order as the given solution. Because the length of the longest directed path in G'_S is at most $m - 1$, the topological ordering will require at most m layers. $\square$

A.2. Polyhedral Study of P_1

Proposition 2. *The dimension of P_1 is $nm + |R|$.*

Proof. The first model has $nm + |R|$ variables, so we claim that P_1 is full-dimensional. Because P_1 contains the origin, it suffices to exhibit $nm + |R|$ linearly independent points in P_1. Index the variables such that the number that corresponds to y_{ip} is $m(i - 1) + p$, and the number that corresponds to x_r is $nm + r$ ($1 \le r \le |R|$). Let e_i be the unit vector in $\mathbb{R}^{nm+|R|}$ with a 1 in the i-th position. The vectors e_i with $i \in \{1, \dots, nm\}$ are linearly independent and belong to P_1. They correspond to setting a single y_{ip} variable to 1. We obtain the remaining $|R|$ points by setting $x_r = y_{d_r 1} = 1$ for each $r \in R$, one at a time. $\square$

Proposition 3. *Given an arc $r \in R$, the inequality $x_r \ge 0$ defines a facet of P_1, whereas the inequality $x_r \le 1$ does not.*

Proof. The origin plus the points described in the proof of Proposition 2, except for the point that has $x_r = 1$, constitute $nm + |R|$ affinely independent points satisfying $x_r = 0$. The inequality $x_r \le 1$ is not facet-defining for P_1 because it is implied by the combination of (2) and (3). $\square$

Proposition 4. *Given a disk $i \in S$, and a level $1 \le p \le m$, the inequality $y_{ip} \ge 0$ defines a facet of P_1, whereas the inequality $y_{ip} \le 1$ does not.*

Proof. Case (i): $p > 1$: the origin plus the points described in the proof of Proposition 2, except for the point $e_{m(i-1)+p}$, constitute $nm + |R|$ affinely independent points that satisfy $y_{ip} = 0$. Case (ii): $p = 1$: use the first nm points from case (i) plus the following points for each $r \in R$: set $x_r = y_{d_r 1} = 1$ when $d_r \neq i$, and set $x_r = y_{d_r 2} = 1$ when $d_r = i$. The inequality $y_{ip} \leq 1$ does not define a facet of P_1 because it is implied by (2). $\square$

Proposition 5. *Given a disk $i \in S$, (2) defines a facet of P_1.*

Proof. We list $nm + |R|$ affinely independent points that satisfy (2) as an equality. The first m points are $e_{m(i-1)+p}$ (i.e. setting $y_{ip} = 1$ for all $1 \leq p \leq m$). The next $nm - m$ points are obtained as follows: by setting $y_{i1} = y_{i'p'} = 1$, for $i' \neq i$ and $2 \leq p' \leq m$, we obtain $(n-1)(m-1)$ points; and by setting $y_{i2} = y_{i'1} = 1$, for $i' \neq i$, we obtain another $n - 1$ points. To obtain the remaining $|R|$ points, for each $r \in R$, first set $x_r = 1$. In addition, if $d_r = i$, set $y_{d_r 1} = 1$; otherwise, set $y_{i1} = y_{d_r 2} = 1$. $\square$

Proposition 6. *Given an arc $r \in R$, (3) defines a facet of P_1.*

Proof. We use the indirect method with generic valid inequality $\pi \vec{x} \leq \pi_0$. Let F be the face of P_1 induced by (3). Because the origin is a feasible solution that satisfies (3) as an equality, we have that $\pi_0 = 0$. Let $1 \leq p \leq m$ and $\vec{x}_{rp}$ satisfy $y_{d_r p} = x_r = 1$, with all other variables equal to zero. It is easy to see that $\vec{x}_{rp}$ is feasible and satisfies (3) as an equality. Then,

$$\pi \vec{x}_{rp} = \pi_{d_r p} + \pi_r = \pi_0 = 0 \ . \tag{22}$$

Therefore, $\pi_{d_r p} = -\pi_r$. By varying the value of p, (22) implies that

$$\pi_{d_r 1} = \pi_{d_r 2} = \cdots = \pi_{d_r m} = -\pi_r = \alpha_r \ . \tag{23}$$

To complete the proof, we need to show that all remaining components of π are equal to zero.

    Let $r' \in R \setminus \{r\}$ with $d_{r'} = d_r$. Consider the vector $\vec{x} = \vec{x}_{rp} + e_{nm+r'}$, whose components are all zero except $y_{d_r p}$, x_r and $x_{r'}$ which have value one. Clearly, $\vec{x}$ is feasible and belongs to F. Therefore, we have $\pi_{r'} = 0$. From now on, let us assume that $d_{r'} \neq d_r$. For any $p \in \{1, \ldots, m\}$, by setting $y_{d_{r'}p} = 1$ and all other variables equal to zero, we obtain a feasible vector $\vec{x}$ that lies on F. As a consequence, $\pi \vec{x} = \pi_0$, implying that $\pi_{d_{r'}p} = 0$ for all $r' \neq r$ and all p. Similarly, choosing $\vec{x}$ such that $y_{d_{r'}p} = x_{r'} = 1$, we generate a feasible point in F which yields $\pi_{r'} = 0$ for all $r' \neq r$. $\square$

Proposition 7. *Given $1 \leq p \leq m$ and $K \in \mathcal{K}$ with $|K| \geq 2$, (4) defines a facet of P_1.*

Proof. We use the indirect method with generic valid inequality $\pi\vec{x} \leq \pi_0$. We partition the variables into five classes and determine the corresponding coefficients in vector π by exhibiting feasible points that satisfy (4) as an equality. (i) y_{jp} with $V(j) \in K$: Let $\vec{x}$ have $y_{jp} = 1$. Then, $\pi\vec{x} = \pi_{jp} = \pi_0$. (ii) y_{jq} with $V(j) \in K$, and $q \neq p$: Let $i \in S$ be such that $V(i) \in K$, and let $\vec{x}$ have $y_{jq} = y_{ip} = 1$. Then, $\pi\vec{x} = \pi_{jq} + \pi_{ip} = \pi_0$, which implies $\pi_{jq} = 0$ because of (i). (iii) y_{jq} with $V(j) \notin K$: There exists $i \in S$ with $V(i) \in K$ such that $V(j)$ is not adjacent to $V(i)$ (otherwise, $V(j)$ would be a vertex of K). For each $1 \leq q \leq m$, let $\vec{x}$ have $y_{jq} = y_{ip} = 1$. Then, as in (ii), $\pi_{jq} = 0$. (iv) x_r with $V(d_r) \in K$: If $\vec{x}$ satisfies $y_{d_rp} = x_r = 1$, we have $\pi\vec{x} = \pi_{d_rp} + \pi_r = \pi_0$, which implies $\pi_r = 0$. (v) x_r with $V(d_r) \notin K$: As in (iii), we can find an $i \in S$ with $V(i) \in K$ such that $V(d_r)$ is not adjacent to $V(i)$. Let $\vec{x}$ have $y_{d_r1} = y_{ip} = x_r = 1$. Then, $\pi\vec{x} = \pi_{d_r1} + \pi_{ip} + \pi_r = \pi_0$, which implies $\pi_r = 0$. $\square$

Proposition 8. *Given an arc $r \in R$, $i \in S_r^I$ and $1 \leq p \leq m$, (5) does not define a facet of P_1, but (13) does if $1 \leq p < m$.*

$$\sum_{a=1}^{p} y_{d_ra} + \sum_{b=p}^{m} y_{ib} + x_r \leq 1 + \sum_{a=1}^{m} y_{d_ra} \qquad (13)$$

Proof. We first show that inequality (5) does not define a facet of P_1. To this end, let $\bar{F}$ denote the face of P_1 induced by (5). Now, we claim that all feasible points in $\bar{F}$ satisfy inequality (2) at equality for $i = d_r$ (otherwise d_r is not assigned to a level, x_r is zero because of (3), and the left-hand side of (5) is at most one). Since P_1 is full-dimensional, $\bar{F}$ cannot be a facet of it.

Notice that, by defining the binary variable $z = \sum_{a=1}^{m} y_{d_ra}$ and lifting this variable in (5), we obtain inequality (13). We now prove that the latter inequality is facet defining for P_1 under the assumptions made in the proposition.

Initially, we observe that (13) is not facet-defining for P_1 when $p = m$ because one can check that it is dominated by one of two valid inequalities presented later in this text (namely (14) and (15)), depending on what kind of arc r is. Moreover, for convenience, we rewrite (13) as:

$$\sum_{b=p}^{m} y_{ib} - \sum_{a=p+1}^{m} y_{d_ra} + x_r \leq 1. \qquad (24)$$

We use the indirect method with generic valid inequality $\pi\vec{x} \leq \pi_0$. We partition the variables into ten classes and establish the appropriate corresponding coefficients in vector π. For each choice of $\vec{x}$ given below, undefined variables are assumed to be equal to zero and the vector is easily shown to be feasible and to lie on the face of P_1 induced by (24). (i) y_{il} for $p \leq l \leq m$: Let $\vec{x}$ have $y_{il} = 1$. Then, $\pi\vec{x} = \pi_{il} = \pi_0$. (ii) y_{jm} for all $j \in S \setminus \{d_r, i\}$: Let $\vec{x}$ have $y_{i(m-1)} = y_{jm} = 1$. Then, $\pi\vec{x} = \pi_{i(m-1)} + \pi_{jm} = \pi_0$ which, from the previous result, implies that $\pi_{jm} = 0$. (iii) y_{jl} for all $j \in S \setminus \{d_r, i\}$ and $1 \leq l \leq m - 1$: Let $\vec{x}$ have $y_{im} = y_{jl} = 1$. Then, $\pi\vec{x} = \pi_{im} + \pi_{jl} = \pi_0$ which, from (i), implies that $\pi_{jl} = 0$. (iv) $y_{d_r l}$ for $1 \leq l \leq p$: Let $\vec{x}$ have $y_{im} = y_{d_r l} = 1$. Then, $\pi\vec{x} = \pi_{im} + \pi_{d_r l} = \pi_0$ which, from (i), implies that $\pi_{d_r l} = 0$. (v) x_r: Let $\vec{x}$ have $y_{d_r p} = x_r = 1$. Then, $\pi\vec{x} = \pi_{d_r p} + \pi_r = \pi_0$ which, from (iv), implies that $\pi_r = \pi_0$. (vi) y_{il} for $1 \leq l \leq p - 1$: Let $\vec{x}$ have $y_{d_r p} = x_r = y_{il} = 1$. Then, $\pi\vec{x} = \pi_{d_r p} + \pi_r + \pi_{il} = \pi_0$ which, from (iv) and (v), implies that $\pi_{il} = 0$. (vii) x_q for all $j \in S \setminus \{d_r, i\}$ and all arcs q of disk j: Let $\vec{x}$ have $y_{i(m-1)} = y_{jm} = x_q = 1$. Then, $\pi\vec{x} = \pi_{i(m-1)} + \pi_{jm} + \pi_q = \pi_0$ which, from (i) and (ii), implies that $\pi_q = 0$. (viii) x_q for all arcs q of disk i: Let $\vec{x}$ have $y_{im} = x_q = 1$. Then, $\pi\vec{x} = \pi_{im} + \pi_q = \pi_0$ which, from (i), implies that $\pi_q = 0$. (ix) x_q for all arcs q of disk d_r except arc r: Let $\vec{x}$ have $y_{d_r p} = x_r = x_q = 1$. Then, $\pi\vec{x} = \pi_{d_r p} + \pi_r + \pi_q = \pi_0$ which, from (iv) and (v), implies that $\pi_q = 0$. (x) $y_{d_r l}$ for $p + 1 \leq l \leq m$: Let $\vec{x}$ have $y_{ip} = y_{d_r l} = x_r = 1$. Then, $\pi\vec{x} = \pi_{ip} + \pi_{d_r l} + \pi_r = \pi_0$ which, from (i) and (v), implies that $\pi_{d_r l} = -\pi_0$. □

A.3. Polyhedral Study of P_2

Proposition 9. *The dimension of P_2 is $n(n - 1) + |R|$.*

Proof. The second model has $n(n-1)+|R|$ variables, so we claim that P_2 is full-dimensional. Because P_2 contains the origin, it suffices to exhibit $n(n-1)+|R|$ linearly independent points in P_2. Index the variables such that the number that corresponds to w_{ij} is $(n-1)(i-1)+j$ when $j < i$ or $(n-1)(i-1)+j-1$ when $j > i$, and the number that corresponds to x_r is $n(n-1)+r$ $(1 \leq r \leq |R|)$. Let e_i be the unit vector in $\mathbb{R}^{n(n-1)+|R|}$ with a 1 in the i-th position. The vectors e_i with $i \in \{1, \ldots, n(n-1)\}$ are linearly independent and belong to P_2. They correspond to setting a single w_{ij} variable to 1. We get the remaining $|R|$ points by setting $x_r = w_{d_r j} = 1$ for each $r \in R$ (one at a time), and $j \in S_r^I$, if any. □

Proposition 10. *Given an arc $r \in R$, the inequality $x_r \geq 0$ defines a facet of P_2, whereas the inequality $x_r \leq 1$ defines a facet of P_2 only when $S_r^I = \emptyset$.*

Proof. The origin plus the points described in the proof of Proposition 9, except for the point that has $x_r = 1$, constitute $n(n-1) + |R|$ affinely independent points satisfying $x_r = 0$. The inequality $x_r \leq 1$ is not facet-defining for P_2 when $S_r^I \neq \emptyset$ because it is implied by (9). If $S_r^I = \emptyset$, we obtain enough affinely independent points satisfying $x_r = 1$ by using the points described in the proof of Proposition 9, except for the origin, and setting $x_r = 1$ in each of them. $\qquad\square$

Proposition 11. *Given two distinct disks $i, j \in S$, the inequality $w_{ij} \geq 0$ defines a facet of P_2 if $S_r^I = \emptyset$ for all arcs r on the border of disk i. Moreover, the inequality $w_{ij} \leq 1$ does not define a facet of P_2.*

Proof. If $S_r^I \neq \emptyset$ for an arc r on the border of i $(d_r = i)$, $w_{ij} \geq 0$ is not facet-defining for P_2 because it is implied by (9). Otherwise, the origin plus the points described in the proof of Proposition 9, except for the point that has $w_{ij} = 1$, constitute $n(n-1) + |R|$ affinely independent points satisfying $w_{ij} = 0$. The inequality $w_{ij} \leq 1$ is not facet-defining for P_2 because it is implied by (8). $\qquad\square$

Proposition 12. *Given two disks $i, j \in S$ with $i < j$, (8) defines a facet of P_2.*

Proof. We use the indirect method with generic valid inequality $\pi \vec{x} \leq \pi_0$. Let $\vec{x}$ have $w_{ij} = 1$. Then, $\pi \vec{x} = \pi_{ij} = \pi_0$. Now let $\vec{x}$ have $w_{ji} = 1$ only. Then, $\pi \vec{x} = \pi_{ji} = \pi_0 = \pi_{ij}$ (from the previous identity). Because of the transitivity constraints (10), we have to take care of the remaining w variables in a specific order. First, we zero out all components of π whose first subindex is i before any others. Specifically, let $\vec{x}$ have $w_{ij} = w_{i\ell} = 1$ for any given $\ell \neq j$. This yields $\pi \vec{x} = \pi_{ij} + \pi_{i\ell} = \pi_0$, which implies $\pi_{i\ell} = 0$ for all $\ell \neq j$. Now define a new $\vec{x}$ by setting $w_{ij} = 1$ and $w_{k\ell} = 1$ for some $(k, \ell) \neq (i, j)$ and $(k, \ell) \neq (j, i)$. If $k \neq j$ we do not have to worry about (10), and this feasible $\vec{x}$ yields $\pi \vec{x} = \pi_{ij} + \pi_{k\ell} = \pi_0$, which implies $\pi_{k\ell} = 0$. If $k = j$, however, $\vec{x}$ also needs to have $w_{i\ell} = 1$. Therefore, $\pi \vec{x} = \pi_{ij} + \pi_{k\ell} + \pi_{i\ell} = \pi_0$. But since we have previously shown that $\pi_{i\ell} = 0$, this last identity implies that $\pi_{k\ell} = 0$.

   Let $r \in R$ and define $\vec{x}$ by setting $x_r = 1$, and $w_{d_r k} = 1$ for all $k \in S_r^I$. If this assignment sets neither w_{ij} nor w_{ji} to 1, make $w_{ij} = 1$ and, if $i \in S_r^I$, also make $w_{d_r j} = 1$. Then, we have $\pi \vec{x} = \pi_r + \pi_{ab} = \pi_0$, where ab is either ij or ji, which implies $\pi_r = 0$. $\qquad\square$

Proposition 13. *Given an arc $r \in R$ and a disk $j \in S_r^I$, (9) defines a facet of P_2.*

Proof. We use the indirect method with generic valid inequality $\pi\vec{x} \leq \pi_0$. Because the origin satisfies (9) as an equality, $\pi_0 = 0$. Let $\vec{x}$ satisfy $w_{ij'} = 1$ for $i \neq d_r$ or $j' \neq j$, with the remaining variables equal to zero. Then, $\pi_{ij'} = \pi_0 = 0$. Moreover, if $x_r = 1$ and $w_{d_r j'} = 1$ for all $j' \in S_r^I$, we have $\pi\vec{x} = \pi_r + \pi_{d_r j} = \pi_0 = 0$, which implies $\pi_r = -\pi_{d_r j} = \alpha$. It remains to show that $\pi_r' = 0$ for $r' \neq r$. Let $r' \in R$ be such that $d_{r'} \neq d_r$. If $x_{r'} = 1$ and $w_{d_{r'} j'} = 1$ for all $j' \in S_{r'}^I$, we conclude that $\pi_{r'} = 0$. On the other hand, if r' is such that $d_{r'} = d_r$, by setting $x_{r'} = x_r = 1$, and $w_{d_r j'} = 1$ for all $j' \in S_{r'}^I \cup S_r^I$, we also conclude that $\pi_{r'} = 0$. $\square$

Proposition 14. *Given three distinct disks $i, j, k \in S$, (10) defines a facet of P_2.*

Proof. We use the indirect method with generic valid inequality $\pi\vec{x} \leq \pi_0$. Let $\vec{x}$ have $w_{ij} = 1$. This implies that $\pi\vec{x} = \pi_{ij} = \pi_0 = \alpha$. Likewise, if $w_{jk} = 1$, we get $\pi_{jk} = \alpha$. Finally, if $w_{ij} = w_{jk} = w_{ik} = 1$, we have that $\pi_{ik} = -\alpha$.

We now show that all remaining coefficients of π are zero. Let i' and j' not in $\{i, j, k\}$ and let $\vec{x}$ have $w_{i'j'} = w_{ij} = 1$. Then, $\pi\vec{x} = \alpha$ implies $\pi_{i'j'} = 0$. Now, let $\ell \notin \{i, j, k\}$. The point satisfying $w_{\ell i} = w_{jk} = 1$ implies $\pi_{\ell i} = 0$, and the point $w_{i\ell} = w_{jk} = 1$ implies $\pi_{i\ell} = 0$. Likewise, the point $w_{\ell k} = w_{ij} = 1$ implies $\pi_{\ell k} = 0$, and the point $w_{k\ell} = w_{ij} = 1$ implies $\pi_{k\ell} = 0$. Continuing in this fashion, the point $w_{\ell j} = w_{ij} = 1$ implies $\pi_{\ell j} = 0$, and the point $w_{j\ell} = w_{jk} = 1$ implies $\pi_{j\ell} = 0$. We still need to show that $\pi_{ji} = \pi_{kj} = \pi_{ki} = 0$. The point satisfying $w_{jk} = w_{ji} = 1$ implies $\pi_{ji} = 0$; the point satisfying $w_{ij} = w_{kj} = 1$ implies $\pi_{kj} = 0$, and, finally, the point with $w_{ki} = w_{jk} = w_{ji} = 1$ implies $\pi_{ki} = 0$.

It remains to show that $\pi_r = 0$ for all $r \in R$. If $d_r \notin \{i, j, k\}$, let $x_r = w_{d_r j'} = 1$ for all $j' \in S$, in addition to $w_{ij} = 1$, to get $\pi_r = 0$. If $d_r = i$, let $x_r = w_{ij'} = 1$ for all $j' \in S_r^I$, together with $w_{ij} = 1$, and $w_{jk} = 1$ if $k \in S_r^I$, to get $\pi_r = 0$. If $d_r = j$, let $x_r = w_{jj'} = 1$ for all $j' \in S_r^I$, in addition to $w_{jk} = 1$, to get $\pi_r = 0$. Finally, if $d_r = k$, let $x_r = w_{kj'} = 1$ for all $j' \in S$, together with $w_{ij} = 1$, to obtain $x_r = 0$ (this works even if i and/or j belong to S_r^I). $\square$

A.4.   Relationship Between P_1 and P_2

Let $\widetilde{P}_1$ be the feasible set of the linear relaxation of (2)–(7) and let $\widetilde{P}_2$ be the feasible set of the linear relaxation of (8)–(12). Moreover, let $\widetilde{P}_1^x$ and $\widetilde{P}_2^x$ be the projections of $\widetilde{P}_1$ and $\widetilde{P}_2$ onto the x-space, respectively. More specifically, $\widetilde{P}_1^x = \{x \in \mathbb{R}^{|R|} \mid (y, x) \in \widetilde{P}_1 \text{ for some } y \in \mathbb{R}^{nm}\}$ and $\widetilde{P}_2^x = \{x \in \mathbb{R}^{|R|} \mid (w, x) \in \widetilde{P}_2 \text{ for some } w \in \mathbb{R}^{n(n-1)}\}$.
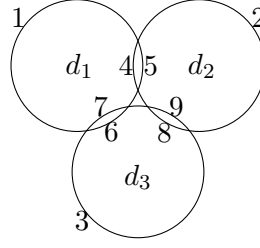
Figure 8: Counterexample showing that $\widetilde{P}_1^x \not\subseteq \widetilde{P}_2^x$.

Proposition 15. $\widetilde{P}_1^x \not\subseteq \widetilde{P}_2^x$.

Proof. We exhibit a fractional solution $(y^0, x^0) \in \widetilde{P}_1$ for which there exists no $w^0 \in \mathbb{R}^{n(n-1)}$ such that $(w^0, x^0) \in \widetilde{P}_2$. Consider the arrangement shown in Figure 8.

The nine arcs in the arrangement are identified by the numbers 1 through 9 (note that $d_1 = d_5 = d_6$, $d_2 = d_4 = d_8$, $d_3 = d_7 = d_9$, and arcs 1, 2, and 3 have two pieces). Therefore, we have $S = \{d_1, d_2, d_3\}$, $R = \{1, \ldots, 9\}$, $m = 3$, and the set of G_S maximal cliques $\mathcal{K}$ is $\{\{d_1, d_2\}, \{d_2, d_3\}, \{d_1, d_3\}\}$. The following solution is feasible for $\widetilde{P}_1$: $x^0 = (\frac{7}{8}, \frac{7}{8}, \frac{7}{8}, \frac{1}{4}, \frac{3}{4}, \frac{1}{8}, \frac{7}{8}, \frac{7}{8}, \frac{1}{8})$, $y_{d_1 1}^0 = y_{d_2 3}^0 = y_{d_3 2}^0 = \frac{3}{8}$, and for all the remaining (disk,level) pairs (i, p), with $i \in S$ and $1 \leq p \leq 3$, let $y_{ip}^0 = \frac{1}{4}$. Feasibility can be checked by substituting these variable values into constraints (2)–(5). Hence, $x^0 \in \widetilde{P}_1^x$. To show that x^0 does not belong to $\widetilde{P}_2^x$ we show that, after substituting x^0 into constraints (9), we cannot find a corresponding vector w^0 that would satisfy (8)–(10). This vector w^0 would have to satisfy $w_{d_1 d_2}^0 = \frac{3}{4}$, $w_{d_2 d_1}^0 = \frac{1}{4}$, $w_{d_1 d_3}^0 = w_{d_3 d_2}^0 = \frac{1}{8}$, and $w_{d_3 d_1}^0 = w_{d_2 d_3}^0 = \frac{7}{8}$, which would violate the transitivity constraint $w_{d_1 d_2}^0 + w_{d_2 d_3}^0 - w_{d_1 d_3}^0 \leq 1$. $\qquad\square$

A.5.   Strengthening the ILP Formulations

Proposition 16. *Let f be a face of $\mathcal{A}$ with $|B_f^+| \geq 1$. If $|C_f| \geq 1$ or $|B_f^+| \geq 2$, then (14) defines a facet of P_1.*

$$\sum_{i \in C_f} y_{im} + \sum_{r \in B_f^+} x_r \leq 1 \tag{14}$$

Proof. To prove validity, note that for every arc $r \in B_f^+$, all the arcs in $B_f^+ \setminus \{r\}$ are in the interior of d_r. Therefore, if r is visible, no other arc of $B_f^+ \setminus \{r\}$ can be visible, which implies $\sum_{r \in B_f^+} x_r \leq 1$. Moreover, if a disk in C_f is at the top level (m), we must have

$\sum_{r \in B_f^+} x_r = 0$, so it suffices to show that $\sum_{i \in C_f} y_{im} \leq 1$. Because all the disks in C_f contain f, the corresponding vertices in G_S form a clique. Hence, at most one of those disks can be assigned to level m because of (4), which implies that (14) is valid.

If $|B_f^+| = 0$, (14) is dominated by (4). If $|C_f| = 0$ and $|B_f^+| = 1$, (14) reduces to $x_r \leq 1$, which is not facet-defining due to Proposition 3.

To prove that (14) is facet-defining for P_1 under the assumptions stated in the proposition, we use the indirect method with generic valid inequality $\pi \vec{x} \leq \pi_0$.

Let $r \in B_f^+$, $1 \leq p \leq m$, and let $\vec{x}_{rp}$ satisfy $y_{d_r p} = x_r = 1$, with all other variables equal to zero. Clearly, $\vec{x}_{rp}$ satisfies (14) as an equality, $\vec{x}_{rp} \in P_1$, and

$$\pi \vec{x}_{rp} = \pi_{d_r p} + \pi_r = \pi_0 \ . \tag{25}$$

By varying the value of p, (25) implies that, for any $r \in B_f^+$,

$$\pi_{d_r 1} = \pi_{d_r 2} = \cdots = \pi_{d_r m} = \alpha_r \ . \tag{26}$$

Let $r \in B_f^+$ and $q \notin B_f^+$. If $p_q < p_r \leq m$, let $\vec{x}_{rqp_r p_q}$ satisfy $y_{d_r p_r} = y_{d_q p_q} = x_r = 1$, with all other variables equal to zero. This gives $\pi \vec{x}_{rqp_r p_q} = \pi_{d_r p_r} + \pi_{d_q p_q} + \pi_r = \pi_0 + \pi_{d_q p_q} = \pi_0$ (using (25)), which implies $\pi_{d_q p_q} = 0$. If $p_r < p_q = m$, there are two cases: (i) $d_q \notin C_f$: we can still set $y_{d_r p_r} = y_{d_q m} = x_r = 1$, which yields $\pi_{d_q m} = 0$ as above; (ii) $d_q \in C_f$: setting $y_{d_q m} = 1$ and all remaining variables equal to zero, we conclude that $\pi_{d_q m} = \pi_0$.

We now deal with coefficients of π corresponding to x variables associated with arcs outside B_f^+. Let $q \notin B_f^+$. There are two cases to consider: (i) $d_q \in C_f$: let $\vec{x}_{qm}$ satisfy $y_{d_q m} = x_q = 1$, with all other variables equal to zero. Then, $\pi \vec{x}_{qm} = \pi_{d_q m} + \pi_q = \pi_0 + \pi_q = \pi_0$. Therefore, $\pi_q = 0$; (ii) $d_q \notin C_f$: Take $r \in B_f^+$ and let $\vec{x}_{qr21}$ satisfy $y_{d_q 2} = y_{d_r 1} = x_q = x_r = 1$ (even if $q \in B_f^-$, both q and r will be visible). Then, by (25) and since $\pi_{d_q p_q} = 0$ for $p_q < m$, we obtain $\pi \vec{x}_{qr21} = \pi_{d_q 2} + \pi_{d_r 1} + \pi_q + \pi_r = \pi_0 + \pi_q = \pi_0$. Hence, $\pi_q = 0$.

If $|B_f^+| \geq 2$, let $p_1 > p_2$, r_1 and $r_2 \in B_f^+$ with $r_1 \neq r_2$, and let $\vec{x}_{r_1 r_2 p_1 p_2}$ satisfy $y_{d_{r_1} p_1} = y_{d_{r_2} p_2} = x_{r_1} = 1$, with all other variables equal to zero. Then, $\pi \vec{x}_{r_1 r_2 p_1 p_2} = \pi_{d_{r_1} p_1} + \pi_{d_{r_2} p_2} + \pi_{r_1} = \alpha_{r_1} + \alpha_{r_2} + \pi_{r_1} = \pi_0$, yielding $\alpha_{r_2} = 0$, because of (25) and (26). Moreover, since r_1 and r_2 were chosen arbitrarily, we can conclude that $\alpha_r = 0$ for all $r \in B_f^+$. Consequently, $\pi_r = \pi_0$ for all $r \in B_f^+$. To achieve the same results when $|B_f^+| = 1$, we assume $|C_f| \geq 1$. Let $\vec{x}_{qrm}$ satisfy $y_{d_q m} = y_{d_r (m-1)} = 1$, where $d_q \in C_f$ and $B_f^+ = \{r\}$. Then, $\pi \vec{x}_{qrm} = \pi_{d_q m} + \pi_{d_r (m-1)} = \pi_0 + \pi_{d_r (m-1)} = \pi_0$, which implies $\pi_{d_r (m-1)} = 0$. Consequently, because of (26), $\pi_{d_r p} = 0$ for all p, and $\pi_r = \pi_0$. $\qquad\square$

Proposition 17. *Let f be a face of $\mathcal{A}$ with $|B_f^-| \geq 1$. For each $r \in B_f^-$, (15) defines a facet of P_1.*

$$\sum_{i \in D_f} y_{im} + x_r \leq 1 \tag{15}$$

Proof. The inequality is clearly valid. To prove that (15) is facet-defining for P_1 under the assumptions stated above, we use the indirect method with generic valid inequality $\pi \vec{x} \leq \pi_0$. Let $1 \leq p \leq m$, and let $\vec{x}_{rp}$ satisfy $y_{d_r p} = x_r = 1$. Clearly, $\vec{x}_{rp}$ satisfies (15) as an equality, $\vec{x}_{rp} \in P_1$, and

$$\pi \vec{x}_{rp} = \pi_{d_r p} + \pi_r = \pi_0 \ . \tag{27}$$

By varying the value of p, (27) implies that

$$\pi_{d_r 1} = \pi_{d_r 2} = \cdots = \pi_{d_r m} = \alpha_r \ . \tag{28}$$

Let $q \neq r$. If $p_q < p_r \leq m$, let $\vec{x}_{rqp_r p_q}$ satisfy $y_{d_r p_r} = y_{d_q p_q} = x_r = 1$. This gives $\pi \vec{x}_{rqp_r p_q} = \pi_{d_r p_r} + \pi_{d_q p_q} + \pi_r = \pi_0 + \pi_{d_q p_q} = \pi_0$ (using (27)), which implies $\pi_{d_q p_q} = 0$. If $p_r < p_q = m$, there are two cases: (i) $d_q \notin D_f$: we can still set $y_{d_r p_r} = y_{d_q m} = x_r = 1$, which yields $\pi_{d_q m} = 0$ as above; (ii) $d_q \in D_f$: setting $y_{d_q m} = 1$ we conclude that $\pi_{d_q m} = \pi_0$.

We now deal with coefficients of π corresponding to x variables associated with arcs $q \neq r$. There are two cases to consider: (i) $d_q \in D_f$: let $\vec{x}_{qm}$ satisfy $y_{d_q m} = x_q = 1$. Then, $\pi \vec{x}_{qm} = \pi_{d_q m} + \pi_q = \pi_0 + \pi_q = \pi_0$. Therefore, $\pi_q = 0$; (ii) $d_q \notin D_f$: Let $\vec{x}_{qr21}$ satisfy $y_{d_q 2} = y_{d_r 1} = x_q = x_r = 1$. Then, $\pi \vec{x}_{qr21} = \pi_{d_q 2} + \pi_{d_r 1} + \pi_q + \pi_r = \pi_0 + \pi_q = \pi_0$. Hence, $\pi_q = 0$.

Finally, let $d_q \in D_f$ and let $\vec{x}_{qrm}$ satisfy $y_{d_q m} = y_{d_r (m-1)} = 1$. Then, $\pi \vec{x}_{qrm} = \pi_{d_q m} + \pi_{d_r (m-1)} = \pi_0 + \pi_{d_r (m-1)} = \pi_0$, which implies $\pi_{d_r (m-1)} = 0$. Consequently, because of (28), $\alpha_r = 0$ and $\pi_r = \pi_0$. $\qquad\square$

Proposition 18. *Let K be a maximal clique in G_R with $|K| \geq 3$. Then, (16) defines a facet of P_2.*

$$\sum_{r \in K} x_r \leq 1 \tag{16}$$

Proof. The inequality is clearly valid. To see the connection between (16) and (14) note that, given a face f of $\mathcal{A}$, the arcs in B_f^+ correspond to a clique in G_R, but when $C_f \neq \emptyset$ that clique is not necessarily maximal.

We begin by showing that (16) does not necessarily define a facet of P_2 when $|K| < 3$. If $|K| = 1$, (16) reduces to $x_r \leq 1$, which may or may not be facet defining, according to Proposition 10. If $|K| = 2$, let r_1 and r_2 be the two arcs of K. The following system of inequalities has to be satisfied:

$$x_{r_1} + x_{r_2} \leq 1 \tag{29}$$

$$w_{d_{r_1} d_{r_2}} + w_{d_{r_2} d_{r_1}} \leq 1 \tag{30}$$

$$x_{r_1} \leq w_{d_{r_1} d_{r_2}} \tag{31}$$

$$x_{r_2} \leq w_{d_{r_2} d_{r_1}} \tag{32}$$

To satisfy (29) as an equality, we need either $x_{r_1} = 1$ or $x_{r_2} = 1$. If $x_{r_1} = 1$, then (31) implies $w_{d_{r_1} d_{r_2}} = 1$, which in turn implies $w_{d_{r_2} d_{r_1}} = 0$ because of (30). Likewise, $x_{r_2} = 1$ implies $w_{d_{r_2} d_{r_1}} = 1$ and $w_{d_{r_1} d_{r_2}} = 0$. Hence, a point that satisfies (29) as an equality also satisfies (30) as an equality, implying that (29) is not facet-defining.

From now on, we assume that $|K| \geq 3$. We use the indirect method with generic valid inequality $\pi \vec{x} \leq \pi_0$. Before proceeding, we define a standard type of feasible point and two sets of disks as follows. For any $r \in R$ with $S_r^I \neq \emptyset$, define $\vec{x}_r$ as the point having $x_r = w_{d_r j'} = 1$ for all $j' \in S_r^I$. Let I_K be the set of all disks in S that contain an arc of K on their border, that is $I_K = \cup_{r \in K} d_r$. Let D_K be the set of disks in S that contain an arc of K in their interior, that is $D_K = \cup_{r \in K} S_r^I$ (note that $I_K \subseteq D_K$).

If $r \in K$, which implies $S_r^I \neq \emptyset$, note that $\vec{x}_r$ satisfies (16) as an equality and $\pi \vec{x}_r$ gives

$$\pi_r + \sum_{j' \in S_r^I} \pi_{d_r j'} = \pi_0 \ , \tag{33}$$

to which we will refer multiple times during the proof.

We will show that the π_{ij} components of π are equal to zero by breaking the proof down into three cases, depending on the value of i. As we consider each possible case for $i \in S$, we will also look at the arcs r on i's border to prove that either $\pi_r = \pi_0$ (when $r \in K$), or $\pi_r = 0$ (when $r \notin K$). This way, once we go through all disks in S, we will also have gone through all arcs in R.

Case 1: $i \in I_K$. This is equivalent to saying that $i = d_r$ for a given $r \in K$. Therefore, we have to show that $\pi_{d_r j} = 0$ for all $j \in S$. We proceed by breaking this case down into three subcases.

Subcase 1.1: $j \notin S_r^I$. Let $\vec{x}$ be initially equal to $\vec{x}_r$ and, in addition, set $w_{d_r j} = 1$. This yields $\pi\vec{x} = \pi\vec{x}_r + \pi_{d_r j} = \pi_0$, which implies $\pi_{d_r j} = 0$ because of (33).

Subcase 1.2: $j \in S_r^I \cap I_K$. This means $j = d_{r_2}$ for some $r_2 \in K \setminus \{r\}$. By assumption, $|K \setminus \{r\}| \geq 2$. Therefore, let $\vec{x}$ be initially equal to $\vec{x}_r$ and, in addition, set $w_{d_{r_2} d_{r_3}} = 1$ for some pair of arcs $r_2, r_3 \in K \setminus \{r\}$. As in Case 1.1, this point yields $\pi_{d_{r_2} d_{r_3}} = 0$ because of (33), and in a similar manner we can also show that $\pi_{d_{r_3} d_{r_2}} = 0$. Note that by repeating the previous argument, we can show that $\pi_{d_r d_{r_3}} = \pi_{d_{r_3} d_r} = 0$ by using $\vec{x}_{r_2}$ as a starting point for $\vec{x}$. Similarly, we can show that $\pi_{d_r d_{r_2}} = \pi_{d_{r_2} d_r} = 0$ by using $\vec{x}_{r_3}$ as a starting point for $\vec{x}$, and so on.

Subcase 1.3: $j \in S_r^I \setminus I_K$. Let $r_2 \in K \setminus \{r\}$ and let $\vec{x}$ be initially equal to $\vec{x}_{r_2}$. Note that the point $\vec{x}_{r_2}$ has $w_{d_{r_2} d_r} = 1$ because $d_r \in S_{r_2}^I$. If $j \in S_{r_2}^I$, $\vec{x}_{r_2}$ also has $w_{d_{r_2} j} = 1$; otherwise we already know that $\pi_{d_{r_2} j} = 0$ (from Subcase 1.1) and we can still set $w_{d_{r_2} j} = 1$ in $\vec{x}$. Either way, observe that it is feasible to also set $w_{d_r j} = 1$ in $\vec{x}$ without violating the transitivity constraint. Then, we have $\pi\vec{x} = \pi\vec{x}_{r_2} + \pi_{d_r j} = \pi_0$, which implies $\pi_{d_r j} = 0$ because of (33).

To conclude the proof of Case 1, we consider arcs r on the border of disks $i \in I_K$ (i.e. $d_r = i$). If $r \in K$, because we have just shown that $\pi_{d_r j} = \pi_{ij} = 0$ for all $j \in S$, (33) implies that $\pi_r = \pi_0$. If $r \notin K$, there exists an arc $r' \in K$ on the border of i so that $d_{r'} = d_r = i$. Notice that from the previous cases we already know that $\pi_{d_r j} = 0$ for all $j \in S - \{d_r\}$. Hence, let $\vec{x}$ be initially equal to $\vec{x}_r + \vec{x}_{r'}$ and, in addition, set $w_{d_{r'} j} = 1$ for all $j \in S_r^I$. Then, $\pi\vec{x} = \pi_r + \pi_{r'} = \pi_0$, which implies $\pi_r = 0$.

Case 2: $i \in S \setminus D_K$. Let $\vec{x}$ be initially equal to $\vec{x}_r$ for some $r \in K$ and, in addition, set $w_{ij} = 1$ for any $j \in S \setminus \{d_r\}$. Then $\pi\vec{x} = \pi\vec{x}_r + \pi_{ij} = \pi_0$, which implies that $\pi_{ij} = 0$. To show that $\pi_{id_r} = 0$, we proceed in a similar way, but start with the point $\vec{x}_{r_2}$ for some $r_2 \in K \setminus \{r\}$ and additionally set $w_{id_r} = 1$.

We now consider the arcs on the border of disks i in this case. Given $r \in K$ and an arc r_1 on the border of i ($d_{r_1} = i$) two subcases may occur:

Subcase 2.1: $d_r \notin S_{r_1}^I$. Use $\vec{x} = \vec{x}_r + \vec{x}_{r_1}$ to get $\pi\vec{x} = \pi_r + \pi_{r_1} = \pi_0$, which yields $\pi_{r_1} = 0$.

Subcase 2.2: $d_r \in S_{r_1}^I$. Start with $\vec{x} = \vec{x}_r + \vec{x}_{r_1}$ and, in addition, also set $w_{ij} = 1$ for all $j \in S_r^I$ to conclude that $\pi_{r_1} = 0$.

Case 3: $i \in D_K \setminus I_K$. This means that i contains some (maybe even all) of the arcs of K in its interior, but no arc of K is on i's border. Given $r \in K$ and $j \in S \setminus \{d_r\}$, to show that $\pi_{ij} = 0$ we can start with the point $\vec{x}_r$, set $w_{ij} = 1$, and set $w_{d_r j} = 1$ (recall that we have already shown that $\pi_{d_r j} = 0$ in Case 1). To show that $\pi_{id_r} = 0$, we begin with the point $\vec{x}_{r_2}$ for some $r_2 \in K \setminus \{r\}$ and additionally set $w_{id_r} = 1$. Note that this works regardless of whether $S_{r_2}^I$ contains i or not, because $\vec{x}_{r_2}$ sets $w_{d_{r_2} d_r} = 1$.

We now consider the arcs on the border of disks i in this case. Given an arc r_1 on the border of i ($d_{r_1} = i$), because $r_1 \notin K$, there exists an arc $r \in K$ such that $d_r \notin S_{r_1}^I$. Therefore, take the point $\vec{x}_r + \vec{x}_{r_1}$ and additionally set $w_{d_r j} = 1$ for all $j \in S_{r_1}^I$. Multiplying this point with π yields $\pi_r + \pi_{r_1} = \pi_0$, which implies $\pi_{r_1} = 0$. □

Proposition 19. *Let $D_S = (V, A)$ be a complete directed graph with one node in V for every disk in S. As before, $V(i)$ denotes the node corresponding to disk i, and an arc from $V(i)$ to $V(j)$ in D_S corresponds to the variable w_{ij}. Let $C = (V(i_1), \ldots, V(i_k), V(i_{k+1}))$, with $i_{k+1} = i_1$ and $i_{k+2} = i_2$, be an odd cycle of length k in D_S. Then, (17) defines a facet of P_2.*

$$\sum_{a=1}^{k} w_{i_a i_{a+1}} - \sum_{a=1}^{k} w_{i_a i_{a+2}} \leq \frac{k-1}{2} \tag{17}$$

Proof. We use the indirect method with generic valid inequality $\pi \vec{x} \leq \pi_0$. We will show that $\pi_{i_a i_{a+1}} = \alpha$ and $\pi_{i_a i_{a+2}} = -\alpha$, for $a = 1, ..., k$, and $\pi_0 = \alpha \frac{k-1}{2}$.

Let $V(i_a)$ be a vertex of C. We refer to subsequent vertices in the directed cycle as $V(i_{a+j})$, for $j = 1, \ldots, k-1$. If $a+j > k$, $i_{a+j} = i_{((a+j) \mod k)}$. Define the point $\vec{x}_{i_a}$ by setting variables $w_{i_{a+j'} i_{a+j'+1}} = 1$ for all j' odd, that is, $w_{i_{a+1} i_{a+2}} = w_{i_{a+3} i_{a+4}} = \ldots = w_{i_{a-2} i_{a-1}} = 1$, as exemplified in Figure 9(i). Note that $\vec{x}_{i_a}$ is feasible and satisfies (17) as an equality. Therefore, $\pi \vec{x}_{i_a} = \pi_0$.

We divide variables w_{ij}, with $i, j \in S$ into four classes. If $V(i), V(j) \notin C$, start with the point $\vec{x}_{i_a}$ and also set $w_{ij} = 1$. When we multiply the resulting point by π, we obtain $\pi \vec{x}_{i_a} + \pi_{ij} = \pi_0$, which implies that $\pi_{ij} = 0$. If $V(i) \in C$ and $V(j) \notin C$, choose a' such that $V(i_{a'}) = V(i)$, start with $\vec{x}_{i_{a'}}$, and additionally set $w_{ij} = 1$ to conclude that $\pi_{ij} = 0$. By proceeding in an analogous way, we can also show that $\pi_{ij} = 0$ when $V(i) \notin C$ and $V(j) \in C$. Next, we deal with the case in which both $V(i)$ and $V(j)$ belong to C.
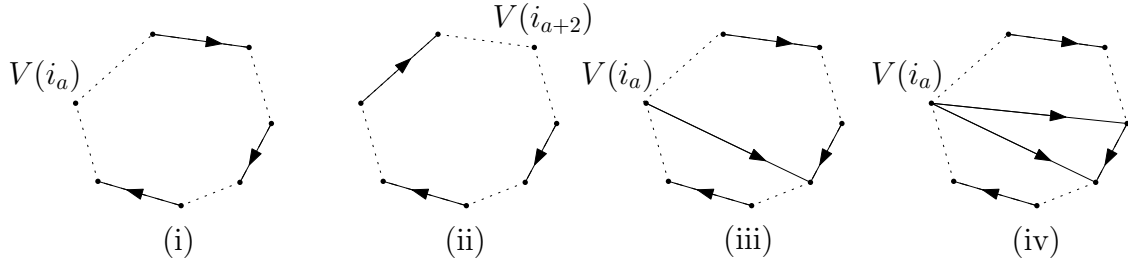
Figure 9: A cycle of length 7. Only edges whose corresponding variable w is set to 1 are shown.

Consider the point $\vec{x}_{i_{a+2}}$; it has $w_{i_{a+3}i_{a+4}} = \cdots = w_{i_{a-2}i_{a-1}} = w_{i_a i_{a+1}} = 1$. Because both $\vec{x}_{i_a}$ and $\vec{x}_{i_{a+2}}$ satisfy (17) as an equality, and the only variables that are equal to one in only one of these points are $w_{i_{a+1}i_{a+2}}$ (in $\vec{x}_{i_a}$) and $w_{i_a i_{a+1}}$ (in $\vec{x}_{i_{a+2}}$), as shown in Figure 9(i) and (ii), it is true that $\pi(\vec{x}_{i_a} - \vec{x}_{i_{a+2}}) = \pi_{i_{a+1}i_{a+2}} - \pi_{i_a i_{a+1}} = 0$. By varying the value of a, we can show that $\pi_{i_a i_{a+1}} = \alpha$ for $a = 1, \ldots, k$. In addition, because $\pi \vec{x}_{i_a} = \pi_0$, we also conclude that $\pi_0 = \alpha \frac{k-1}{2}$.

If we take the point $\vec{x}_{i_a}$ and also set $w_{i_a i_{a+1}} = w_{i_a i_{a+2}} = 1$ for $a = 1, \ldots, k$, it is easy to see that the resulting point is feasible and still satisfies (17) as an equality. Since $\pi \vec{x}_{i_a} = \pi_0$, we conclude that $\pi_{i_a i_{a+1}} + \pi_{i_a i_{a+2}} = 0$. Therefore, $\pi_{i_a i_{a+2}} = -\pi_{i_a i_{a+1}} = -\alpha$, for all $a = 1, \ldots, k$.

We now show that $\pi_{i_a i_b} = 0$ for $b \neq a + 1$ and $b \neq a + 2$, for all $a = 1, \ldots, k$. Start with the point $\vec{x}_{i_a}$. Let $a' = a + j'$, with $j' \geq 3$ and odd. Recall from the definition of $\vec{x}_{i_a}$ that $w_{i_{a'}i_{a'+1}} = 1$. Then, set $w_{i_a i_{a'+1}} = 1$, as shown in Figure 9(iii) and multiply the resulting point by π to conclude that $\pi_{i_a i_{a'+1}} = 0$ for all a'. Now create another point starting with $\vec{x}_{i_a}$ and setting $w_{i_a i_{a'}} = 1$. To respect the transitivity constraint (10), we also have to set $w_{i_a i_{a'+1}} = 1$, as shown in Figure 9(iv). As before, we conclude that $\pi_{i_a i_{a'}} = 0$ for all a'.

Finally, we consider the π_r components of π, for each $r \in R$. If $V(d_r) \notin C$, start with the point $\vec{x}_{i_a}$ for an arbitrary $i_a \in C$. Otherwise, start with the point $\vec{x}_{i_a}$ with $i_a = d_r$. Next, define $\vec{x}$ as the point $\vec{x}_{i_a}$ chosen in the previous step, with the following additional components set to one: $x_r = 1$ and $w_{d_r j} = 1$ for all $j \in S$.

If $V(d_r) \notin C$, no other variable in (17) has been set to one in $\vec{x}$ besides those in $\vec{x}_{i_a}$. Therefore, $\pi \vec{x} = \pi_0$ allows us to conclude that $\pi_r = 0$.

If $V(d_r) \in C$, the resulting point $\vec{x}$ sets only two additional variables in (17) to one, namely $w_{i_a i_{a+1}}$ and $w_{i_a, i_{a+2}}$. Nevertheless, the equality between the left-hand side and the right-hand side of (17) is maintained because the coefficients of those variables have opposite signs. Therefore, $\pi \vec{x} = \pi_0$ also allows us to conclude that $\pi_r = 0$. $\square$

A.6.   Decomposition Techniques

Proposition 20. *Let S be a set of disks such that G_S is not 2-connected and let v be a disk corresponding to an articulation point of G_S. Let S_k contain v plus the disk set of the k-th connected component obtained after the removal of $V(v)$ from G_S. The optimal solutions for each S_k can be combined into an optimal solution for S in polynomial time.*

Proof. Let $V(v)$ be an articulation point of G_S and let v be its corresponding disk in S (note that articulation points can be found in $O(|E|)$ time, Cormen et al., 2001). Using the notation introduced in the proposition, consider the disk subsets S_i and S_j corresponding to any two distinct connected components of $G_S - V(v)$. By definition, the pieces of v's border contained in $S_i \setminus \{v\}$ and in $S_j \setminus \{v\}$ are disjoint. Hence, the optimal solutions of the problems defined over S_i and S_j do not influence each other. In other words, the relative order imposed by those solutions onto the disks of each such subset is optimal for the complete set of disks S. If we consider these orders as representing an orientation of the arcs of G_S, we have a directed acyclic graph G'_S. The optimal assignment of disks to levels can be obtained in polynomial time from a topological ordering of G'_S.   □

Proposition 21. *Let S be a set of disks and let H_S be a directed graph with one node for every disk in S and an arc from node i to node j whenever a portion of the border of i's disk is contained in the interior of j's disk. Let S_k be the disk set of the k-th strongly connected component of H_S. The optimal solutions for each S_k can be combined into an optimal solution for S in polynomial time.*

Proof. Let I and J be two distinct strongly connected components of H_S, and let S_I and S_J be their corresponding sets of disks, respectively. Either there exists no directed arc between I and J — in which case they can be solved independently — or, without loss of generality, all arcs go from I to J. (Having arcs in both directions would imply that I and J form a single strongly connected component.) In the latter case, there exists a disk $d_I \in S_I$ that is entirely contained inside some disk $d_J \in S_J$. As a consequence, every disk in S_I must be entirely contained inside d_J. To see why, suppose that there exists $d'_I \in S_I$ disjoint from d_J. Because d_I and d'_I belong to the same strongly connected component, there must exist another disk $d''_I \in S_I$ crossing the border of d_J, as shown in Figure 10, which would contradict the fact that I and J are distinct components. Hence, because S_I is entirely contained inside
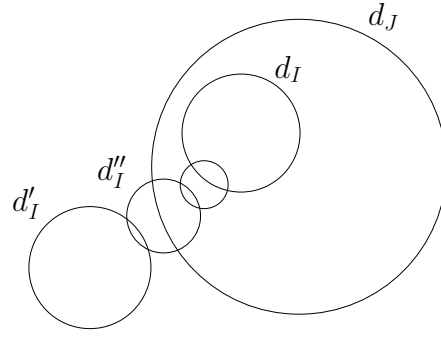
Figure 10: If d_I is contained in d_J and d'_I is disjoint from d_J, there must exist a disk d''_I that crosses the border of d_J, which leads to a contradiction.

a disk of S_J, we can independently calculate the optimal solutions to these two sets of disks and then draw all the disks that belong to S_I on top of the disks that belong to S_J.   □